Journal of Solid State Chemistry 184 (2011) 2108–2113

Contents lists available at ScienceDirect

Journal of Solid State Chemistry

journal homepage: www.elsevier.com/locate/jssc

The fluorite–pyrochlore transformation of $Ho_{2-y}Nd_yZr_2O_7$

Richard Clements [a,b], James R. Hester [a], Brendan J. Kennedy [b,*], Chris D. Ling [a], Anton P.J. Stampfl [a,b]

[a] School of Chemistry, The University of Sydney, Sydney, NSW 2006, Australia
[b] Bragg Institute, Australian Nuclear Science and Technology Organisation, Lucas Heights, NSW 2234, Australia

ARTICLE INFO

Article history:
Received 8 March 2011
Received in revised form
21 May 2011
Accepted 30 May 2011
Available online 6 June 2011

Keywords:
Pyrochlore structure
Fluorite structure
Oxide pyrochlores
Defect chemistry
Disorder transformation
Neutron diffraction

ABSTRACT

Twelve members of the $Ho_{2-y}Nd_yZr_2O_7$ series, prepared using conventional solid state methods, have been characterised by neutron powder diffraction. $Ho_2Zr_2O_7$ has a defect fluorite structure whereas $Nd_2Zr_2O_7$ is found to adopt the ordered pyrochlore structure with the composition induced fluorite–pyrochlore transformation occurring near $y=1$. Rietveld analysis on the neutron data for all the compositions reveals an increase in lattice parameter as a function of y across the entire series, with a small discontinuity associated with the transformation. The neutron profile results suggest that domains of pyrochlore-type initially begin to form before crystallising into a separate phase, and therefore that anion and cation ordering processes are distinct. There is a strong correlation between the extent of disorder in the anion sublattice and the x-parameter of 48*f* oxygen. These results point the way to a better understanding of the stability observed in pyrochlore structures.

1. Introduction

The remarkable stability of the pyrochlore structure type allows for numerous chemically distinct materials to be prepared, some of which display properties that are technologically important including catalytic activity, piezoelectricity, ferro- and ferrimagnetism, luminescence and giant magnetoresistance [1,2] The electronic properties of pyrochlores vary from being superconducting, metallic, or semiconducting to having a high ionic conductivity [2].

Lanthanide zirconates, $Ln_2Zr_2O_7$, are being developed for use in solid oxide fuel cells [3], in thermal barrier coatings (TBCs) that are employed to extend the practical lifetime of devices such as turbine blades as well as allowing these to operate at higher temperatures [4] and for the storage of nuclear waste [5,6]. While the titanate pyrochlores transform to an amorphous structure upon irradiation, the zirconate pyrochlores remain crystalline to very high doses [5]. The effect of ion bombardment on tin pyrochlores has also been studied [6].

Pyrochlore oxides have the general formula $A_2B_2X_6Y$, where *A*, *B* are cations and *X*, *Y* are anions. Most pyrochlore oxides ($X=Y=$oxygen) crystallise in space group $Fd\bar{3}m$ (#227). Of the four possible choices of origin in this space group, the most commonly used places the smaller *B*-type cation at the 16*c* site with the larger *A*-type cation at 16*d*. There are two anion sites, with O (or *X*) at 48*f*, and O′ (or *Y*) at 8*b*. There are only two variable structural parameters, the cubic lattice parameter, *a*, and the positional parameter, *x*, for the O atom in 48*f*. The pyrochlore structure can be described in several ways, most commonly as interpenetrating BX_6 octahedra and A_2Y chains [1,7]. The structure may also be described as an anion deficient fluorite, since the coordination polyhedra around the *A* and *B* cations change shape with the value of the O 48*f* positional parameter, *x*. In the pyrochlore phase, the smaller *B*-type cation is coordinated to the six O-type anions in a distorted octahedron. The larger *A*-type cation is in a distorted cube that is best described as consisting of a puckered six membered ring of O atoms with two O′ atoms forming linear O′–*A*–O′ chains, reminiscent of the Cu_2O structure, that are normal to the average plane of the six-membered ring [1]. The *A*–O and *A*–O′ bond distances are very different. Typically the *A*–O distances are around 2.4–2.5 Å, in accord with the sum of the ionic radii, whilst the *A*–O bonds are among the shortest known for any rare-earth oxide, ~2.2 Å. Vacancies in the A_2O' are relatively common, and even when the *A*-site is fully occupied the O′ anion site (8*b*) may be only partially occupied. The pyrochlore structure can also be considered as a fluorite superstructure in which the 8*a* sites are vacant and there is an ordering of the two cations. A final description of the structure depicts the cations at the 16*c* and 16*d* sites forming a three-dimensional array of corner-sharing tetrahedra, where both types of cations are magnetic giving rise to a geometrically frustrated lattice [2]. The fluorite structure is in space group $Fm\bar{3}m$ and since both the cations and anions occupy general positions it does not have any variable atomic positional parameters.

* Corresponding author. Fax: +61 2-9351 3329.
E-mail address: B.Kennedy@chem.usyd.edu.au (B.J. Kennedy).

0022-4596/$ - see front matter © 2011 Elsevier Inc. All rights reserved.
doi:10.1016/j.jssc.2011.05.054

In the pyrochlore structure the presence of a lone-pair active *A* cation, such as Pb^{2+} or Bi^{3+}, results in off centring, through incoherent local displacements of the *A*-type cation, which can couple with the disorder of the anions. As a consequence of the relatively weak interaction between the B_2O_6 and A_2O sublattices of the pyrochlore [1] the structure can tolerate a large degree of substitutional [8] and displacive disorder on the *A*-cation site [9,10].

Naively the stability of the pyrochlore superstructure in the lanthanide zirconates may be thought to be linked to the ratio of the *Ln* and Zr cation radii [11–13]. It is now well established that when the lanthanide radius is larger than Gd, the ordered pyrochlore structure is generally encountered, while the smaller and hence higher *f*-electron containing lanthanides form fluorite-type structures [1]. Under certain conditions, including high temperature or after ion beam irradiation, the *Ln* and Zr cations are disordered over the *A* and *B* sites, and 48*f*, 8*b* and the normally unoccupied 8*a* anion sites can be occupied by both anions and vacancies [1]. Under extreme conditions an order–disorder transition from the pyrochlore to defect-fluorite structure is observed [14]. This transition is a very rare example of simultaneous disordering of both anions and cations. Those oxides with *Ln*=Nd–Gd all display a pyrochlore–fluorite transition upon heating with the transition temperature rapidly decreasing as the ionic radii of the lanthanide cation decreases and number of 4*f*-electrons increase from 2300 °C in $Nd_2Zr_2O_7$ to 1530 °C in $Gd_2Zr_2O_7$ [15]. Complex transformations can also occur upon the application of pressure [16].

There have been numerous studies of the effect of chemical substitution on the structural transformation from the perfect pyrochlore to defect fluorite [17–19]. This transformation can be induced by substitution at the *B*-site as illustrated by the work of Glerup et al. [20] on the series $Y_2Ti_{2-y}Zr_yO_7$. A feature of this work was the observation of an intermediate disordered phase. Mandal et al. [21] studied the same transformation in $Nd_{2-y}Y_yZr_2O_7$ series. Given the importance of the anion disorder in the transformation it is surprising that very few neutron diffraction studies of this transformation have been reported. Two notable exceptions are the early work of Heremans et al. [22] on $Y_2Ti_{2-y}Zr_yO_7$ and the recent study of Whittle et al. [23] on $Y_{1.2}La_{0.8}Zr_2O_7$. A further challenge in the study of the pyrochlore to defect fluorite transformation in the zirconates is that it occurs near *Ln*=Gd. Gd has an extremely large thermal neutron absorption coefficient 49,700 barn for $\lambda=1.798$ Å that effectively precludes neutron diffraction studies.

The aim of the present work is to establish if anion disorder existed in the pyrochlore type zirconates poised near the fluorite–pyrochlore transformation, and if so what if any correlation existed between the disorder in the anion sublattice and the *x*-parameter of 48*f* oxygen in the pyrochlore phase. To do this a number of samples of the type $Ho_{2-y}Nd_yZr_2O_7$ were prepared and their structures examined using high resolution powder neutron diffraction.

2. Experimental

Twelve samples in the series $Ho_{2-y}Nd_yZr_2O_7$ ($0 \le y \le 2$) were prepared using conventional solid state methods. The appropriate stoichiometric quantities of Ho_2O_3, Nd_2O_3 and ZrO_2 (calcined at 1000 °C overnight before use), sufficient to prepare ~20 g of material, were finely mixed before being fired at 1200 °C for 24 h. The resulting powders were then re-ground, under acetone, for 10 min in an agate jar in a planetary ball mill at 350 rpm for 15 min. The ground powders were hydrostatically pressed into rods and heated at 1450 °C for 85 h. This process was then repeated to yield single phase samples as established using a Shimadzu S-6000 X-ray diffractometer. Scanning Electron Micrographs were measured using a Carl Zeiss Evo 50 scanning electron microscope with LaB_6 filament operated at 25 kV equipped with an IXRF System energy dispersive spectroscopy (EDS) detector (EDS2006 version 1.0). The exception was the sample of $Nd_2Zr_2O_7$ used in the synchrotron measurements, which was found to contain a small amount of Nd_2O_3. This was not evident in the neutron diffraction profile of this material.

Neutron powder diffraction (NPD) data were obtained over the angular range $10 < 2\theta < 160^\circ$ using the high resolution powder diffractometer Echidna at ANSTO's OPAL facility at Lucas Heights [24]. The wavelength of the incident neutrons, obtained using a Ge (331) monochromator, was 1.299 Å. For these measurements the sample was contained in a 12 mm diameter vanadium can. Synchrotron X-ray powder diffraction (S-XRD) data were collected at ambient temperature in the angular range $5 < 2\theta < 85^\circ$, using X-rays of wavelength 0.94814 Å on the powder diffractometer at

Table 1
The results of the Rietveld refinements for the $Ho_{2-y}Nd_yZr_2O_7$ series as a function of composition. Selected bond-distance are given. The structures were refined using neutron diffraction data measured with $\lambda=1.299$ Å.

y	2.0	1.8	1.6	1.4	1.2	1.1	1.0[a]	0.9	0.6	0.4	0.2	0.0
a	10.6424(1)	10.6049(2)	10.5871(1)	10.5652(2)	10.5607(3)	10.5563(3)	10.5093(3)	5.2521(1)	5.2429(1)	5.2317(2)	5.2283(1)	5.2213(2)
x	0.3365(1)	0.3406(3)	0.3396(2)	0.3409(2)	0.3419(3)	0.3402(4)	0.3516(5)					
NdU11	1.76(5)	1.36(7)	1.27(3)	1.27(4)	1.63(6)	1.30(7)	2.35(15)	2.12(3)	2.29(3)	2.20(3)	1.92(2)	2.28(3)
U12	0.29(3)	0.29(10)	0.31(4)	0.35(5)	0.27(8)		0.04(18)					
Zr11	1.31(3)	0.39(2)	2.13(5)	2.43(6)	3.11(11)	2.66(13)	2.22(17)					
Zr12	0.15(4)	0.06(2)	0.36(6)	0.54(9)	0.53(16)		0.03(20)					
O111	2.31(5)	4.20(21)	3.13(8)	3.32(11)	4.6(2)	2.78(11)	7.8(4)	5.89(7)	5.88(7)	5.31(6)	5.24(6)	5.40(7)
O122	1.30(3)	1.78(9)	2.11(5)	2.37(6)	2.81(10)		3.89(14)					
O123	0.32(5)	0.46(13)	0.63(6)	0.82(8)	0.98(14)		1.5(2)					
O211	1.25(6)	2.40(22)	1.30(7)	1.48(10)	1.84(17)	1.38(15)	3.6(4)					
Nd–O(1)	2.5626(9)	2.525(2)	2.525(2)	2.513(1)	2.504(2)	2.515(2)	2.426(3)	2.2742(1)	2.2703(1)	2.2655(1)	2.2639(1)	2.2609(1)
Nd–O(2)	2.3041(1)	2.2959(1)	2.2922(1)	2.2874(1)	2.2865(1)	2.2855(1)	2.2753(1)					
Zr–O(1)	2.0945(6)	2.106(1)	2.100(1)	2.100(10)	2.104(2)	2.095(1)	2.142(3)					
*n*8*a*	0.0061(5)	0.008(1)	0.010(1)	0.0123(8)	0.0115(12)	0.006(1)	0.0182(19)					
R_p	4.68	7.71	4.57	4.37	5.76	4.33	5.52	5.82	4.25	5.16	5.66	5.14
R_{wp}	6.01	10.35	5.94	5.53	7.50	5.44	7.07	7.40	5.40	6.56	7.21	6.59
χ^2	1.97	7.12	2.37	1.26	2.16	1.38	2.73	3.51	2.55	2.73	3.35	2.72

[a] This sample contained both pyrochlore and fluorite phases. The refined lattice parameter for the fluorite phase was 5.26056(16).

BL-10 of the Australian Synchrotron [25]. The sample was placed in a 0.2 mm diameter capillary that was rotated during the measurements.

The structure was refined using the Rietveld method implemented in the programme Rietica [26]. The neutron peak shape was modelled using a pseudo Voigt function convoluted from asymmetry resulting from axial divergence and the background was estimated using a fourth-order polynomial in 2θ, which was refined simultaneously with the other profile and structural parameters. Anisotropic atomic displacement parameters (ADPs) were refined as allowed by symmetry. No correction was applied for the moderate neutron absorption of the Nd or Ho cations. These refinements are summarised in Table 1. The peak shape in the synchrotron data was modelled using a pseudo-Voigt function and the background was estimated using a linear interpolation between a set of 40 background points.

3. Results and discussion

Probing the fluorite–pyrochlore structure in the $Ln_2Zr_2O_7$ lanthanide zirconates is hindered by a lack of precise structural studies. The presence of very heavy *Ln* and Zr atoms limits the precision with which XRD techniques can be used to characterise the O atom array. NDP is generally used to solve this problem. Unfortunately, however, the strong neutron absorption of Gd effectively precludes using neutron diffraction methods unless the sample is enriched in a non-absorbing isotope of Gd [27], yet it is around $Gd_2Zr_2O_7$ that the transformation occurs. The strategy employed here is to examine solid solutions of the type $Ho_{2-y}Nd_yZr_2O_7$. Assuming the lanthanide can be considered as predominantly ionic in character then it is reasonable to model Gd^{3+} by a mixture of larger and smaller lanthanides. The choice of Ho and Nd was made, based on their relative sizes, neutron absorption coefficients and the knowledge that they always adopt a single stable oxidation state ($+3$), whereas alternate lanthanides such as Pr or Tb can adopt either $+3$ or $+4$ oxidation states. High quality samples of this series were readily prepared using conventional solid state methods. The colour of these changed from pale yellow in $Ho_2Zr_2O_7$ to dull purple-red in $Nd_2Zr_2O_7$ under fluorescent lighting. Neither XRD nor electron microscopy provided any evidence for any impurities in the materials.

Representative examples of the NPD profiles for a pyrochlore and fluorite type oxide are shown in Fig. 1. As noted above, the pyrochlore can be viewed as a superstructure of the fluorite cell with the cubic lattice parameters $a_p \sim 2a_f$. This gives rise to additional reflections in the pyrochlore phase, the strongest of which are the $\langle 331 \rangle$ and $\langle 511 \rangle$ at $2\theta \sim 30.5^\circ$ and 37°, respectively, for $\lambda = 1.299$ Å. A striking feature of the NPD profiles is the obvious diffuse-type scattering in the fluorite-type phases, most apparent in the low angle region of the profile, with the background in the pattern of $Ho_2Zr_2O_7$ increasing noticeably at low angles. This is not observed in the S-XRD profiles, (Fig. 2), demonstrating that it is associated with oxygen order/disorder rather than local ordering of the cations. Whilst the fluorite–pyrochlore transition shows obviously first-order kinetics, the presence of weak and relatively broad Bragg reflections corresponding to a doubling of the cell length in the NPD pattern of the $y=1$ sample ($HoNdZr_2O_7$), in which there is no evidence for cation ordering, provides the first conclusive proof for the suggestion of Heremans [22] that the anion ordering process is distinct from that of the cations. That is the transformation commences with the growth of anion ordered domains, followed by the cation ordering. Diffuse scattering has previously been observed in a number of related systems including cation doped $Y_{0.15}Zr_{0.85}O_{1.93}$ fluorite type phases, indicating the presence of partial or short-range ordering of the oxygen vacancies, as well as in the closely related $Y_{2-y}La_yZr_2O_7$ pyrochlore oxides [28].

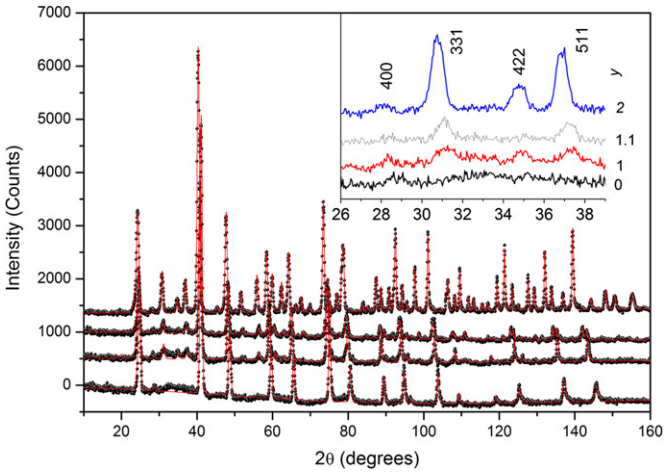

Fig. 1. NPD profiles for selected members in the series $Ho_{2-y}Nd_yZr_2O_7$ {$Nd_2Zr_2O_7$ ($y=2$), $Nd_{1.1}Ho_{0.9}Zr_2O_7$ ($y=1$) $NdHoZr_2O_7$ ($y=1.1$) and $Ho_2Zr_2O_7$ ($y=0$)}, illustrating the transformation from the ordered pyrochlore structure to the disordered fluorite structure. Note the increase in the background intensity at low angles in the fluorite phase. The data are represented by the symbols and the solid lines are the results of the Rietveld analysis. The inset highlights both the appearance of selected superlattice reflections (indexed here on the pyrochlore cell; the pyrochlore (400) reflection corresponds to the fluorite (200) reflection) and the diffuse background in the Ho-doped samples.

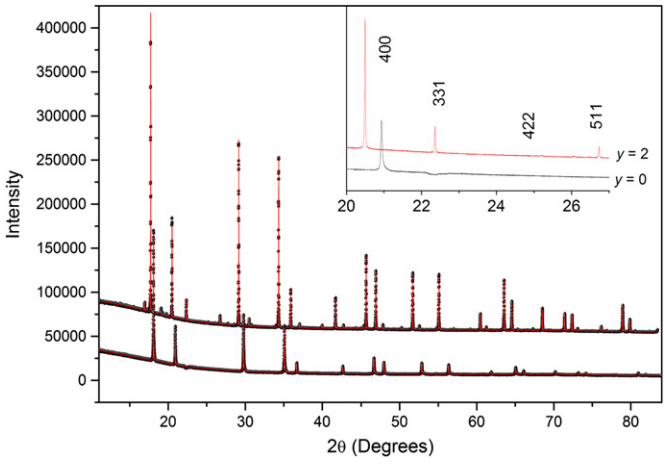

Fig. 2. S-XRD profiles for the end members $y=2$ ($Nd_2Zr_2O_7$) and $y=0$ ($Ho_2Zr_2O_7$) in the series $Ho_{2-y}Nd_yZr_2O_7$, illustrating the transformation from the ordered pyrochlore structure to the disordered fluorite structure. The data are represented by the symbols and the solid lines are the results of the Rietveld analysis. Both phases show a similar increase in background intensity at low angles. The inset highlights both the appearance of selected superlattice reflections (indexed here on the pyrochlore cell) and the absence of appreciable diffuse scattering in the Ho sample. The weak unfitted peaks in the $Nd_2Zr_2O_7$ pattern are from an Nd_2O_3 impurity.

The NPD profile for the sample of nominal composition $Ho_{0.9}Nd_{1.1}Zr_2O_7$ showed the co-existence of both the fluorite and the pyrochlore phases and a satisfactory fit to the experimental profile was only obtained when both phases were included in the refinements. Examination of the experimental profiles showed a well-resolved doublet near $2\theta = 135^\circ$, corresponding to the $\langle 642 \rangle$ fluorite and $\langle 1284 \rangle$ pyrochlore-type reflections, both of which are required by symmetry to be perfectly overlapped by single peaks in cubic symmetry. Rietveld refinements give a composition ratio of 60.0(2.5)% pyrochlore. This was the only composition where there was any experimental evidence, in the form of either resolved peak splitting or broadening, for the two phases co-existing in appreciable

amounts. A sample of composition $Y_{1.2}La_{0.8}Zr_2O_7$ has been reported to contain approximately equal proportions of pyrochlore and defect fluorite phases [23]. Co-existence of the two phases has also been observed in $Nd_{2-y}Y_yZr_2O_7$ [21] and this is clearly a feature of such systems.

Allowing partial occupancy of the nominally vacant 8*a* site during the refinement of the structure of $Nd_2Zr_2O_7$ resulted in a small improvement in the quality of the fit. χ^2 decreased from 2.07% to 1.94% with the refined occupancy of the 8*a* site being 11(1)%. In an early NPD study, van Dirk suggested that while it is appropriate to consider stoichiometric $Nd_2Zr_2O_7$ as a perfect pyrochlore it is likely that this contains a small number ($<5\%$) of intrinsic oxygen defects [29]. The authors are unaware of any other previous reports of anion disorder in $Nd_2Zr_2O_7$, although a small amount of anion disorder has also been observed in undoped $Nd_2Hf_2O_7$ [30]; Zr and Hf oxides generally exhibit very similar crystal chemistry, in part due to the lanthanide contraction. Increasing the amount of Ho in the sample results in an increase in the O occupancy of the 8*a* site to a maximum value of 33(3)% in $HoNdZr_2O_7$, although, again, the reduction in χ^2 resulting from this additional parameter is small, in this case decreasing from 2.90% to 2.70%. Whittle et al. [23] has noted an increase in the extent of anion disorder in the closely related $La_{2-y}Y_yZr_2O_7$ oxides and found a maximum occupancy of the 8*a* site of 17% near the pyrochlore–fluorite transition. The extent of disorder is clearly greater in the present system, however we cannot establish if this indicates a significant difference between the two systems or if it reflects differences in the conditions used to prepare the samples, although the latter explanation appears more likely [23]. The degree of disorder is apparently correlated with the observed *x*-coordinate of the oxygen on the 48*f* position (Fig. 3) with the *x*-coordinate moving towards the value seen in the fluorite structure (0.375) as the extent of disorder increases [31]. A similar trend appears in the small number of $La_{2-x}Y_xZr_2O_7$ samples studied by Whittle et al. [23]. Finally it should be noted that the 442 reflection was not observed in any of the present neutron diffraction patterns. The 442 reflection is a systematic absence for $Fd\bar{3}m$ when the Wyckoff sites *a*–*d* and *f* are occupied but when atoms occupy in any other site this additional extinction does not hold [32]. In pyrochlores with the so-called lone pair active ions on the *A* site, such as in $Bi_2Ti_2O_7$ [33] or in the series $Bi_{2-y}Yb_2Ru_2O_7$ [9], the 442 reflection is evident in the neutron profiles as a consequence of cation disorder from the 16*d* to the 96*g* sites. At the same time O is partially distributed over the 32*e* sites.

In brief the NPD data show that anion disorder occurs across the entire $Ho_{2-y}Nd_yZr_2O_7$ series. Anion disorder is a feature of the defect fluorites ($Ho_2Zr_2O_7$ can be written as defect fluorite with the formula $(Ho_{0.5}Zr_{0.5})O_{1.75}$ highlighting the presence of anion vacancies) and is associated with the favourable ionic conductivity of such oxides [34]. The cation ordered (pyrochlore) and disordered (fluorite) phases co-exist over a narrow composition range and demonstrate that anion and cation ordering events need not occur simultaneously.

The composition dependence of the unit cell parameters for the 12 members of the $Ho_{2-y}Nd_yZr_2O_7$ series is illustrated in Fig. 4. The lattice parameter for the pyrochlore phase, a_p, is noticeably larger than twice that of the fluorite phase, a_f. The increased volume of the pyrochlore phase is believed to be due to anion ordering and has been observed previously in the series $Ln_2Zr_2O_7$. Not unexpectedly, gradual replacement of the Ho^{3+} (ionic radius for 8-coordinate cation [35] IR=1.015 Å) with the larger Nd^{3+} (IR=1.109 Å) cation results in an expansion in the cubic lattice parameter in both the ordered pyrochlore and the disordered fluorite phase, although this is clearly non-linear in the pyrochlore phase. There are two features of Fig. 4 that are worthy of discussion. Firstly the neutron diffraction pattern of the sample with $y=1.0$ shows well-resolved superlattice reflections, indicative of a pyrochlore phase, at low angles but not at high angles. Irrespective of whether a fluorite or pyrochlore model is used in the analysis of this data the lattice parameter falls on the trend line expected for the fluorite-type phases. Evidently this sample could be described as fluorite-type but with domains where ordering of the anions, but not the cations, occurs. The profile for the $y=1.1$ sample demonstrates the co-existence of the two phases. Given the "pyrochlore-like", anion ordering observed in the sample with $y=1.0$, it is likely that at this composition cation ordering has commenced but there remain appreciable domains within the sample where this is not present. The significance of the non-linear increase of the lattice parameter of the pyrochlore phase is not clear. As already described the sample with $y=1.1$ is two-phase and the possibility that the

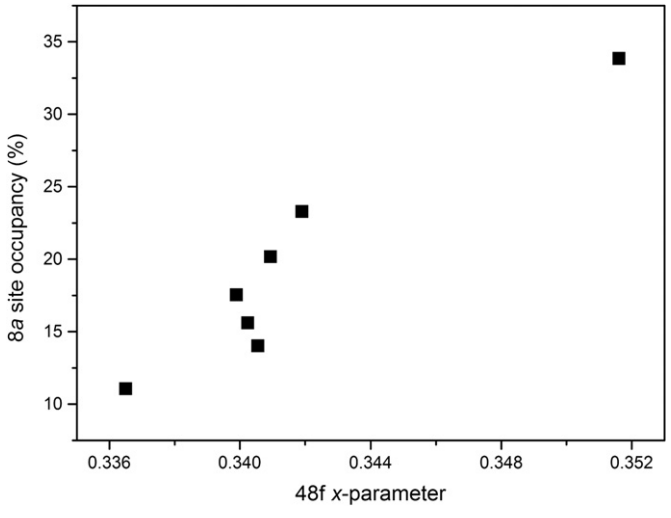

Fig. 3. Plot of the position of the oxygen on the 48*f* site in the pyrochlore and the extent of occupancy of the 8*a* site for the seven pyrochlore samples found in the series $Ho_{2-y}Nd_yZr_2O_7$. The extent of disorder appears to increase as the oxygen positional parameter increases, reflecting a shift to the fluorite structure.

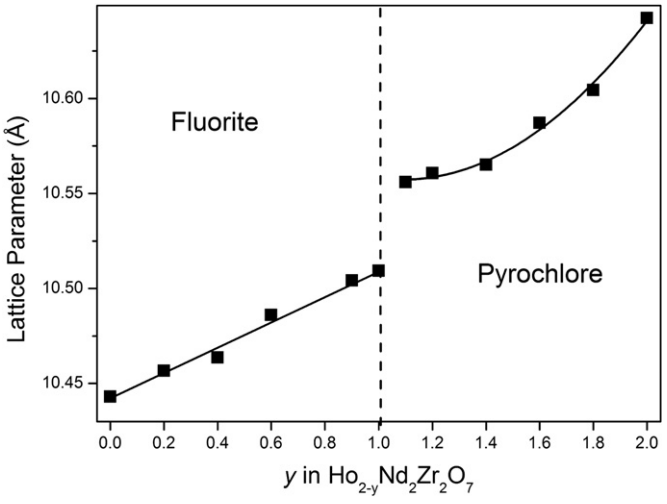

Fig. 4. Composition dependence of the unit cell parameters of the series $Ho_{2-y}Nd_yZr_2O_7$ established by Rietveld refinement against NPD data. The dotted vertical line shows the approximate transition point. The sample at $y=1.1$ contains around 40% fluorite phase. The solid lines serve as a guide to the eye and demonstrate the discontinuous volume change associated with the pyrochlore–fluorite transformation.

effective composition of the pyrochlore phase is different to that of the bulk material cannot be excluded. Whilst there is no clear evidence in the form of resolved peaks or systematic broadening in the NPD profile of the sample with $y=1.2$, it is possible that a small amount of fluorite phase is present in this sample and this may impact on the refined lattice parameters, and it is tempting to conclude that the non-linear behaviour reflects fine-scale phase separation. Whittle et al. [23] reached a similar conclusion in their study of $La_{2-x}Y_xZr_2O_7$. Irrespective of the cause, the expansion of the pyrochlore phase is clearly anomalous near the transformation, with the expected linear-like (Vegard's Law) behaviour only seen remote from this.

The order–disorder transition occurs near $y=1$, corresponding to an effective ionic radius of 1.062 Å. The critical value established here is similar, but not identical, to that seen when a single lanthanide is used with $Gd_2Zr_2O_7$ (IR=1.053 Å) having a pyrochlore structure and "$Tb_2Zr_2O_7$" (IR=1.04 Å) adopting the disordered fluorite structure. It should be noted that $Gd_2Zr_2O_7$ undergoes a transformation to the disordered fluorite structure near 1530 °C [15]. This transformation appears to be sensitive to the precise composition [36,37] and it also appears that the additional disorder inherent in the doped system acts to favour the formation of the fluorite phase. In this regard, it is interesting to note the report by Lee and co-workers that the fluorite phase of $Gd_2Zr_2O_7$ could be obtained using a polymeric citrate precursor method followed by calcinations at relatively low temperatures (700–1200°), whereas the higher temperatures used to prepare samples using conventional methods yield the pyrochlore structure [38]. Complex oxides prepared using low temperatures synthetic methods are expected to have greater disorder, see, for example, ref. [23].

A significant advantage of using neutron, rather than X-ray diffraction, is the improved accuracy and precision in determining the value of the variable positional parameter of the 48*f* oxygen atoms, Table 1. This affords an accurate measure of the *Ln*–O and Zr–O bond distances; the composition dependencies of these are illustrated in Fig. 5. The average Zr–O distance shows a small but apparently significant decrease as the amount of Ho incorporated into the sample increases. Obviously in the fluorite phase this reflects the disorder of the lanthanide and zirconium cations, where the effective ionic radius of the metal site is decreasing with increase in Ho content. The small reduction in Zr–O distance observed in the pyrochlore phase is thought to be a consequence of competition between the bonding requirements of the *Ln* and Zr cations, inducing a systematic increase in the single variable oxygen positional parameter as the lattice parameter decreases. A similar trend has been observed in the tin pyrochlores $Ln_2Sn_2O_7$ [39].

The quality of the NPD data was such that it was possible to refine anisotropic ADPs for the four types of atoms in the pyrochlore-type structures. The environment of the oxygen atoms on the 48*f* site (*C*2*v* site symmetry) is distorted having two nearest *Ln* and two more distant *Ln* neighbours. In this case movement along the Zr–O–Zr chains (given by $U_{22}-U_{23}$) is always smaller than that perpendicular to the chain in either the [100] or [011] directions (given by U_{11} and $U_{22}+U_{23}$, respectively) [40]. The oxygen atoms on the 8*b*, and partially occupied 8*a*, site are required by symmetry to have isotropic ADPs. Likewise, the displacement of the *Ln* cations is highly anisotropic with displacement towards to two closest O′ atoms ($U_{11}+2U_{12}$) being noticeably smaller than the displacement perpendicular to this ($U_{11}-U_{12}$). There was no evidence from NPD for any displacive disorder of the *Ln* cations. As noted above such disorder is commonly observed where the *A*-site cation contains lone pair electron [10], but has also been seen in $La_2Zr_2O_7$ [41].

The isotropic ADPs for oxygen atoms (Fig. 6) are relatively independent of composition across the fluorite phase, but then shows a step-like decrease at the transformation to the pyrochlore phase. There appears to be a general softening of the structure with increased disorder, as found by Heremans in $Y_2Ti_{2-y}Zr_yO_7$ [22]. The fact that the ADP are greater in the fluorite phase than in the pyrochlore phase reflects the larger number of vacancies in the former case. The magnitude of these displacements is consistent with the numerous reports of high ionic conductivity in fluorite-type zirconates. There are of course two types of oxygen atoms in the pyrochlore phase: the APDs of the O_2 atoms on the 8*b* sites do not exhibit any systematic variation on composition; however those for the O1 atoms on the 48*f* site are systematically reduced as the Nd content increases. This result is consistent with the hypothesis that the most stable oxygen defect involves the formation of vacancies on the 48*f* O site as suggested in the early work of van Dijk et al. [42].

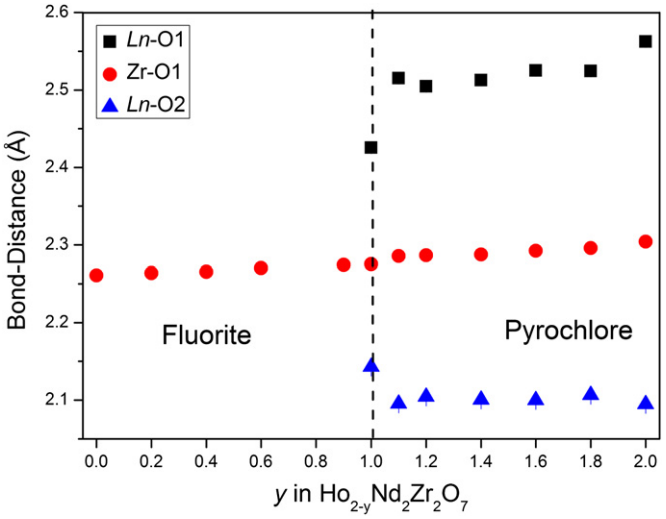

Fig. 5. Composition dependence of the Zr–O and *Ln*–O bond distances in the series $Ho_{2-y}Nd_yZr_2O_7$ established by Rietveld refinement against NPD data. In the fluorite phase the Zr and *Ln* cations occupy the same site, therefore there is only one M–O distance.

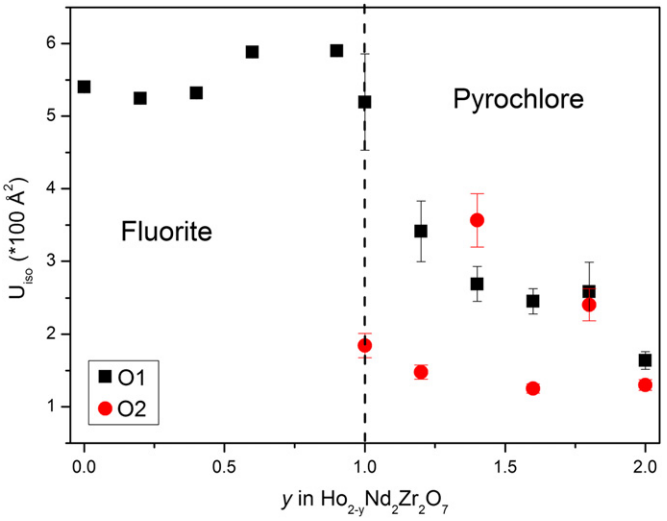

Fig. 6. Composition dependence of the isotropic ADPs for the anions in the series $Ho_{2-y}Nd_yZr_2O_7$ established by Rietveld refinement against NPD data, illustrating the increase accompanying the transition to the fluorite structure at higher Ho contents.

4. Conclusion

This work shows through the use of high resolution NPD data that $Ho_2Zr_2O_7$ has a defect fluorite structure where the Ho and Zr cations are statistically disordered onto the 4*a* site and the oxygen anions partially occupy the 8*c* site. There is clear evidence for diffuse scattering in the neutron diffraction profile of this, and the other fluorite phases studied, as a consequence of anion mobility. Partially replacing the Ho with the larger Nd cation in solid solutions of the type $Ho_{2-y}Nd_yZr_2O_7$ initially simply results in an increase in the cubic lattice parameter. The structured background in the NPD profiles is, at low Nd contents, relatively unaffected. On further doping with Nd, some structure appears in the diffuse background as a consequence of ordering of the vacancies in the anion sublattice. At the critical composition y–1, domains of the cation-ordered pyrochlore phase appear, and over a narrow composition range the pyrochlore and fluorite phases co-exist. This is accompanied by a non-linear increase in the lattice parameters in the pyrochlore phase, possibly indicative of the fine-scale phase separation, as suggested to occur in $La_{2-x}Y_xZr_2O_7$ by Whittle et al. [23]. Such an anomaly is not evident in recent studies of $Sm_{1-x}Yb_xZr_2O_7$ [43] or $Sm_{2-x}Dy_xZr_2O_7$ [44], and it needs to be established if this is a consequence of the smaller number of samples examined in that work. The data provides conclusive proof that the anion ordering process is distinct from that of the cations as was suggested by Heremans et al. [22]. Further increasing the Nd content results in a single-phase pyrochlore-type material; however, Rietveld refinement against NPD data demonstrates partial disorder of the anions persists in this phase. There appears to be a correlation between the composition, the 48*f* positional parameter and the extent of anion disorder in the pyrochlore-type phase. A similar trend appears in the small number of $La_{2-x}Y_xZr_2O_7$ samples studied by Whittle et al. [23].

Acknowledgments

RC thanks ANSTO for the award of a post-graduate scholarship. This work was, in part, performed on the powder diffraction beamline at the Australian Synchrotron. BJK and CDL acknowledge the support of the Australian Research Council.

References

[1] M.A. Subramanian, G. Aravamudan, G.V.S. Rao, Progress in Solid State Chemistry 15 (1983) 55.
[2] M.T. Weller, R.W. Hughes, J. Rooke, C.S. Knee, J. Reading, Dalton Transactions (2004) 3032.
[3] D.J.L. Brett, A. Atkinson, N.P. Brandon, S.J. Skinner, Chemical Society Reviews 37 (2008) 1568.
[4] X.Q. Cao, Journal of Materials Science & Technology 23 (2007) 15.
[5] R.C. Ewing, W.J. Weber, J. Lian, Journal of Applied Physics 95 (2004) 5949.
[6] J. Lian, K.B. Helean, B.J. Kennedy, L.M. Wang, A. Navrotsky, R.C. Ewing, Journal of Physical Chemistry B 110 (2006) 2343.
[7] B.C. Chakoumakos, Journal of Solid State Chemistry 53 (1984) 120.
[8] T.A. Vanderah, I. Levin, M.W. Lufaso, European Journal of Inorganic Chemistry 2005 (2005) 2895.
[9] L.Q. Li, B.J. Kennedy, Chemistry of Materials 15 (2003) 4060.
[10] W. Somphon, V. Ting, Y. Liu, R.L. Withers, Q. Zhou, B.J. Kennedy, Journal of Solid State Chemistry 179 (2006) 2495.
[11] L. Cai, A.L. Arias, J.C. Nino, Journal of Materials Chemistry 21 (2011) 3611.
[12] H. Yamamura, H. Nishino, K. Kakinuma, K. Nomura, Solid State Ionics 158 (2003) 359.
[13] B. Wuensch, K. Eberman, JOM Journal of the Minerals, Metals and Materials Society 52 (2000) 19.
[14] D. Michel, M. Perezyjo., R. Collongu., Materials Research Bulletin 9 (1974) 1457.
[15] D. Michel, M. Perez y Jorba, R. Collongues, Materials Research Bulletin 9 (1974) 1457.
[16] F.X. Zhang, M. Lang, Z.X. Liu, R.C. Ewing, Physical Review Letters (2010) 105.
[17] A.N. Radhakrishnan, P.P. Rao, K.S. Sibi, M. Deepa, P. Koshy, Journal of Solid State Chemistry 182 (2009) 2312.
[18] B.P. Mandal, A. Banerji, V. Sathe, S.K. Deb, A.K. Tyagi, Journal of Solid State Chemistry 180 (2007) 2643.
[19] Y. Liu, R.L. Withers, L. Noren, Journal of Solid State Chemistry 177 (2004) 4404.
[20] M. Glerup, O.F. Nielsen, F.W. Poulsen, Journal of Solid State Chemistry 160 (2001) 25.
[21] B.P. Mandal, P.S.R. Krishna, A.K. Tyagi, Journal of Solid State Chemistry 183 (2010) 41.
[22] C. Heremans, B.J. Wuensch, J.K. Stalick, E. Prince, Journal of Solid State Chemistry 117 (1995) 108.
[23] K.R. Whittle, L.M.D. Cranswick, S.A.T. Redfern, I.P. Swainson, G.R. Lumpkin, Journal of Solid State Chemistry 182 (2009) 442.
[24] K.D. Liss, B. Hunter, M. Hagen, T. Noakes, S. Kennedy, Physica B—Condensed Matter 385-86 (2006) 1010.
[25] K.S. Wallwork, B.J. Kennedy, D. Wang, AIP Conference Proceedings, vol. 879, 2007, p. 879.
[26] B.A. Hunter, C.J. Howard, RIETICA, Lucas Heights Research Laboratories, Sydney, 1998.
[27] B.J. Kennedy, Q.D. Zhou, M. Avdeev, Journal of Solid State Chemistry, in press, doi:10.1016/j.jssc.2011.04.003.
[28] S. Garcia-Martin, M.A. Alario-Franco, D.P. Fagg, J.T.S. Irvine, Journal of Materials Chemistry 15 (2005) 1903.
[29] T. Van Dijk, R.B. Helmholdt, A.J. Burggraaf, Physica Status Solidi (b) 101 (1980) 765.
[30] R. Ubic, I. Abrahams, Y. Hu, Journal of the American Ceramic Society 91 (2008) 235.
[31] L. Minervini, R.W. Grimes, K.E. Sickafus, Journal of the American Ceramic Society 83 (2000) 1873.
[32] J.E. Greedan, D. Gout, A.D. Lozano-Gorrin, S. Derahkshan, T. Proffen, H.J. Kim, E. Bozcaronin, S.J.L. Billinge, Physical Review B 79 (2009) 014427.
[33] I. Radosavljevic, J.S.O. Evans, A.W. Sleight, Journal of Solid State Chemistry 136 (1998) 63.
[34] J.A. Diaz-Guillen, A.F. Fuentes, M.R. Diaz-Guillen, J.M. Almanza, J. Santamaria, C. Leon, Journal of Power Sources 186 (2009) 349.
[35] R.D. Shannon, Acta Crystallographica Section A 32 (1976) 751.
[36] M. Zinkevich, C. Wang, F.M. Morales, M. Ruhle, F. Aldinger, Journal of Alloys and Compounds 398 (2005) 261.
[37] A.J. Feighery, J.T.S. Irvine, C. Zheng, Journal of Solid State Chemistry 160 (2001) 302.
[38] Y.H. Lee, H.S. Sheu, J.P. Deng, H.C.I. Kao, Journal of Alloys and Compounds 487 (2009) 595.
[39] B.J. Kennedy, B.A. Hunter, C.J. Howard, Journal of Solid State Chemistry 130 (1997) 58.
[40] G.R. Facer, M.M. Elcombe, B.J. Kennedy, Australian Journal of Chemistry 46 (1993) 1897.
[41] Y. Tabira, R.L. Withers, T. Yamada, N. Ishizawa, Zeitschrift Fur Kristallographie 216 (2001) 92.
[42] M.P. van Dijk, A.J. Burggraaf, A.N. Cormack, C.R.A. Catlow, Solid State Ionics 17 (1985) 159.
[43] C. Wan, Z. Qu, A. Du, W. Pan, Journal of the American Ceramic Society 94 (2011) 592.
[44] F.N. Sayad, V. Grover, K. Bhattacharyya, D. Jain, A. Arya, C.G.S. Pillai, A.K. Tyagi, Inorganic Chemistry 50 (2011) 2354.